Applied Surface Science 318 (2014) 309–313

Contents lists available at ScienceDirect

Applied Surface Science

journal homepage: www.elsevier.com/locate/apsusc

Co doping induced structural and optical properties of sol–gel prepared ZnO thin films

Ebru Gungor[a,*], Tayyar Gungor[a], Deniz Caliskan[b], Abdullah Ceylan[c], Ekmel Ozbay[b]

[a] Energy Systems Engineering Department, Mehmet Akif Ersoy University, Burdur 15030, Turkey
[b] Nanotechnology Research Center, Bilkent University, Ankara 06800, Turkey
[c] SNTG Laboratory, Physics Engineering Department, Hacettepe University, Ankara 06800, Turkey

ARTICLE INFO

Article history:
Received 15 November 2013
Received in revised form 14 June 2014
Accepted 20 June 2014
Available online 27 June 2014

Keywords:
ZnO
Co:ZnO
Thin film
Ultrasonic spray pyrolysis

ABSTRACT

The preparation conditions for Co doping process into the ZnO structure were studied by the ultrasonic spray pyrolysis technique. Structural and optical properties of the Co:ZnO thin films as a function of Co concentrations were examined. It was observed that hexagonal wurtzite structure of ZnO is dominant up to the critical value, and after the value, the cubic structural phase of the cobalt oxide appears in the X-ray diffraction patterns. Every band-edge of Co:ZnO films shifts to the lower energies and all are confirmed with the PL measurements. Co substitution in ZnO lattice has been proved by the optical transmittance measurement which is observed as the loss of transmission appearing in specific region due to Co^{2+} characteristic transitions.

1. Introduction

Zinc oxide (ZnO) is a II–VI compound semiconductor with a wide direct band gap of 3.37 eV at room temperature. In addition to the electrical and optical properties of undoped ZnO, the transition metal doped ZnO forms are promising candidate materials in the field of spintronics (spin-electronics). Various methods such as pulsed laser deposition [1], chemical vapor transport [2], electrodeposition [3], co-precipitation [4] and solid-state reaction [5], and spray pyrolysis [6] can be used to synthesize ZnO. Among these methods, spray pyrolysis technique can be applicable without vacuum environment; of course, this technique is cheap and displaying comparable properties and competitive functionality with that produced by other techniques. The research has been increased on the ternary semiconductors such as transition metal doped ZnO owing to its high Curie temperature for the ferromagnetic transition calculated in bulk materials and found to be around 300 K [7–10].

Co doping creates a considerable change in the band gap of ZnO [11–14], but this variation has been reported as an increase in some other research and as a decrease in the band gap for ZnO in other research. This case indicates the uncertainty. A reason for this can be structural defects in the ZnO crystal lattice as well as because of the vacancies in the crystal structure or interstitials [15]. The uncontrolled cases as the structural defects and/or impurities that arise as growing the film affects the bonding nature, charge transfer and the band structure in the material. This makes it very difficult to obtain reproducible device performance and reliability. Some authors reported in the literature that red-shift is attributed to the *sp–d* exchange and some other authors observed that blue-shift is attributed to the Burnstein–Moss effect considering the Co concentration. When the volume solubility limit in two-component and multicomponent alloys has reached a certain concentration, the first phase remains constant and then the extra phases appear. In order to determine the solubility limit, one has to follow the change of the lattice spacing and concentration obtained from the X-ray diffraction (XRD) and SEM-EDS spectrum, respectively. There is uncertainty about solubility limit for Co doped ZnO. Lee et al. [16] reported that the doped Co ion was fully substituted into a ZnO lattice at 5 mol%, but the secondary phase of the Co_3O_4 was formed above 5 mol% of Co doping. However, other reports [17,18] have indicated that Co can be incorporated in the matrix of ZnO up to 7–10 at% without forming any second phase. All these reports thus indicate that Co has a limited solubility in ZnO up to 10 at%. In contrast to this, Rath [19] observed that all the peaks match well with the wurtzite structure of ZnO in both pure and Co doped ZnO samples up to a cobalt concentration of 20%.

In this study, we aimed to contribute to clarify the uncertainty for band gap shift. That is why, we investigate the structural and optical properties of ZnO and Co:ZnO (CZO) thin films that were

* Corresponding author.
E-mail address: egungor@mehmetakif.edu.tr (E. Gungor).

http://dx.doi.org/10.1016/j.apsusc.2014.06.132
0169-4332/

Table 1
The atomic percentage of oxygen, zinc and cobalt in the Co:ZnO thin films obtained from EDS measurements.

Sample name	Molarity of Co (M)	Normalized atomic weight (%)		
		O	Zn	Co
CZO1	0.01	42.6	12.6	3.9
CZO2	0.02	36.9	22.6	2.8
CZO3	0.03	42.4	29.2	12.1
CZO4	0.04	38.6	18.8	12.4
CZO5	0.05	43.6	24.3	13.8

deposited onto glass substrates using the ultrasonic spray pyrolysis (USP) method as a function of Co concentration.

2. Material and methods

ZnO and Co:ZnO (CZO) thin films were deposited on to ultrasonically cleaned glass substrates using the ultrasonic spray pyrolysis (USP) method. For conventional USP method, the substrates are fixed and precursor solution sprayed over a hot substrate. The substrate temperature was kept at 400 °C. The salts of zinc acetate dehydrate ($Zn(CH_3COO)_2{\cdot}2H_2O$, 99.9%-Merck) and cobalt acetate tetrahydrate ($Co(CH_3COO)_2{\cdot}4H_2O$, 99.9%-Merck) were used as the metal sources which were solved in methanol. In order to produce a clear and homogeneous solution monoethanolamine (MEA) and acetic acid were added into the precursor solution which was stirred at 60 °C at a moderate speed for 1 h. In the starting solutions, Co contents were changed from 0.01 M to 0.05 M and samples were labeled as CZO1–CZO5 (Table 1). Zn content (0.05 M) was held at constant. The solution flow rate was held constant at 5 ml/min. Nozzle, 100 kHz oscillator frequency, used in this study was in a downward vertical configuration and the nozzle to substrate distance was 12 cm. Compressed air was used as the carrier gas. The films were deposited for about 10 min. A more detailed description of the method to obtain the thin films and the characteristics of the spray pyrolysis device used were reported in previous paper [6]. X-ray diffraction (XRD) spectra were collected with a D-Max X-ray diffractometer (Rigaku International Corp., Japan) with CuKα ($\lambda = 1.5405$ Å) to obtain the structural information of the films. The chemical composition of the thin films was measured using energy dispersive spectroscopy (EDS) with a Jeol JSM-7000F-EDS electron microscope. The optical measurements of the Co:ZnO thin films were carried out at room temperature using T70 Model Spectrophotometer (PG Instrument) in the wavelength range 300–900 nm. Photoluminescence (PL) spectra were measured using a 100 mW He-Cd laser ($\lambda = 325$ nm) as the excitation source and a HORIBA Jobin-Yvon 1m monochromator.

3. Results and discussion

3.1. Structural properties

The X-ray patterns for Co:ZnO thin films at room temperature and reference peak positions are presented in Fig. 1a. The results pointed out showed that there is no impurity and/or unreacted phase of Zn and Co considering the reference peak positions, (1 0 0), (0 0 2), (1 0 1), and (1 0 3) peaks of ZnO were observed. However, (1 1 1) and (2 0 0) peaks at 36.9° and 42.7° Bragg angle of cobalt oxide, respectively, were observed. The starting molarity up to 0.03 M of precursor solution included Co, (0 0 2) peak of hexagonal wurtzite structure becomes more intensive comparing with other peaks (Fig. 1b). In these films, up to 0.03 M, the hexagonal wurtzite structure of ZnO seems to be protected. In the doping process, it is observed that there is a limitation of Co doping into the ZnO structure. The molarity is then greater and/or equal to the 0.03 M value,

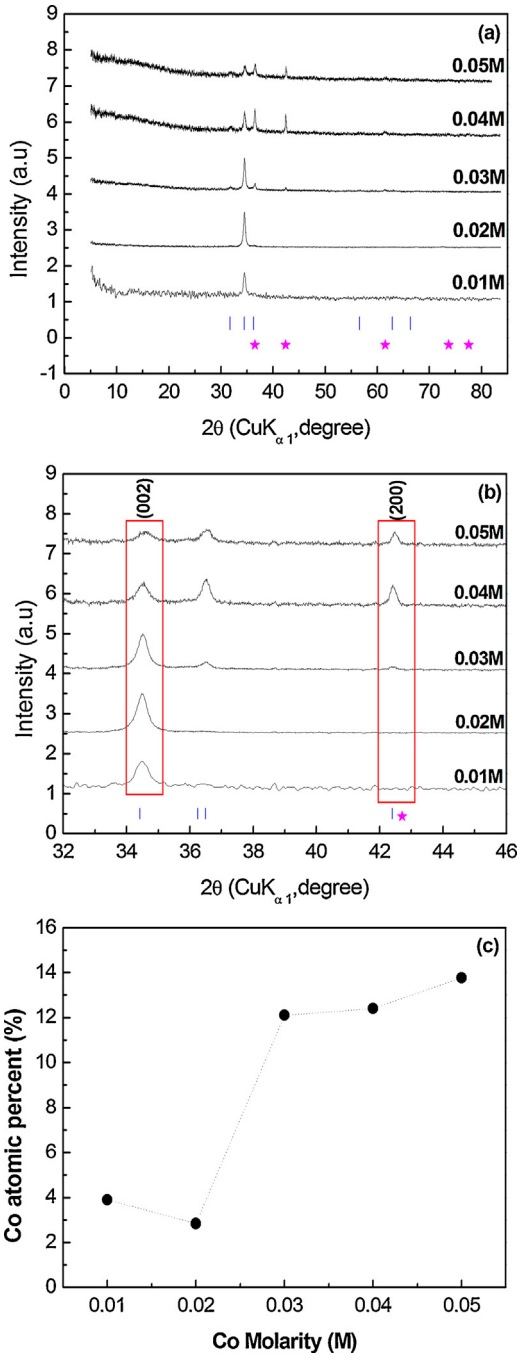

Fig. 1. X-ray diffraction patterns of Co:ZnO thin films (a), and intensity differences of (0 0 2) and (2 0 0) peaks for the films (b).“|” and “⋆” symbols indicate the reference for ZnO (JCPDS 36-1451) and for CoO (JCPDS 43-1004), respectively. The variation of the Co concentration obtained from EDS with starting solution molarity (c).

(2 0 0) peak which belongs to the cubic structure of cobalt oxide which then starts to occur. This limit value is confirmed using EDS measurements. Table 1 summarizes the relative chemical content of the oxygen, zinc and cobalt present in the films as a function of content of the cobalt acetate tetrahydrate inserted in the starting solution. We observed that the Co substituted Zn site up to 12% (Fig. 1c) which corresponded to 0.03 M without showing any extra phase in XRD spectra. Peaks corresponding to the glass substrate elements such as Si and Ca were also detected. The (0 0 2) peak indicating a strong orientation along the *c*-axis of ZnO with hexagonal wurtzite structure is replaced by (2 0 0) orientation with the cubic structure as Co molarity increases. The peak position of (0 0 2) shifts

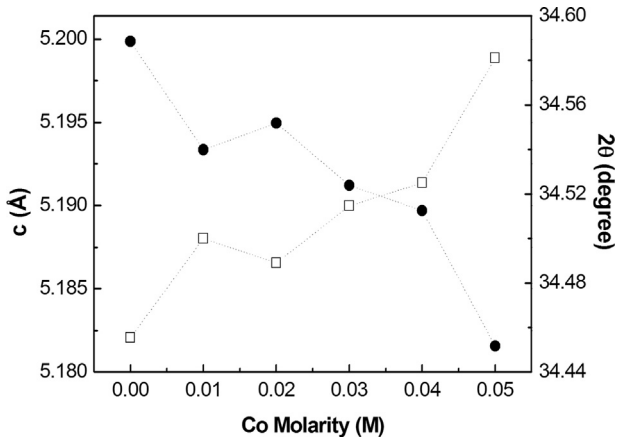

Fig. 2. Structural parameters of Co:ZnO thin films according to the XRD results vs Co molarity; for *c*-lattice parameter ("●" symbol) and diffraction angle 2θ for (0 0 2) peak ("□" symbol).

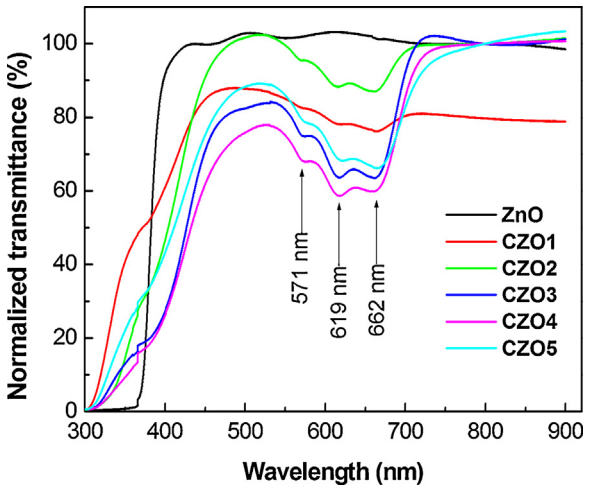

Fig. 3. Normalized experimental optical transmission spectra for Co:ZnO thin films according to transmission value at 800 nm.

to the higher Bragg angle, and also the calculated *c*-lattice parameter decreases due to the increasing of Co concentration in the ZnO structure (Fig. 2). But the intensity of (2 0 0) peak decreases when Co is doped into the ZnO structure with the molarity value of more than 0.04 M.

3.2. Optical properties

The optical transmission spectra of ZnO and Co doped ZnO thin film samples are shown in Fig. 3. The effects of Co doping into the ZnO lattice are clearly observed in the optical transmission spectra. The increase of Co concentration in the ZnO structure decreases the optical transmittance and imparts deep green color to the samples (Fig. 4). In addition, increasing Co concentration also modifies optical transmittance for the specific region due to Co^{2+} characteristic transitions. These transitions also suppress the interference fringes in this region of Co:ZnO films if the film thickness is sufficient to create interference fringe. In order to eliminate the influence of differences in sample thickness, normalized transmittance to the value at 800 nm were taken into account. The absorption peaks, indicated with arrows in Fig. 3, centered at 571 nm (2.18 eV), 619 nm (2.01 eV) and 662 nm (1.88 eV), are related to characteristic features of *d*–*d* transition of Co^{2+} ions. They are assigned to transition from $^4A_2(F)$ state to $^2E(G)$, $^4T_1(P)$ and $^2A_1(G)$ states, respectively [15]. This is a clear evidence to prove the existence of

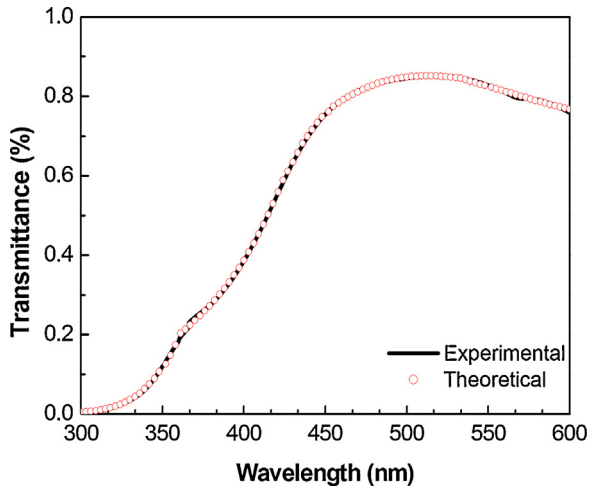

Fig. 4. Experimental optical transmission spectra (solid line) of 0.02 M Co content in starting solution for Co:ZnO thin film: Also the theoretical optical transmission spectra ("o" symbol) are shown for comparison.

Table 2
Calculated film thickness *t* (nm), refractive index *n* for 532 nm wavelength and E_g (eV) optical band gap values of the Co:ZnO (CZO) thin films vs the molarity of Co in the starting solutions.

Sample name	Molarity of Co (M)	*t* (nm)	*n* (532 nm)	E_g (eV)
ZnO	0.00	75 ± 2	1.73	3.330
CZO1	0.01	105 ± 2	2.23	3.072
CZO2	0.02	95 ± 2	2.42	3.061
CZO3	0.03	160 ± 2	2.73	2.985
CZO4	0.04	170 ± 2	2.63	3.020
CZO5	0.05	180 ± 2	2.59	3.030

Co at the tetrahedral sites of the ZnO hexagonal wurtzite structure as Co^{2+}. Comparing the ionic radii of Co^{2+} (0.058 nm) which is very close to ionic radii of Zn^{2+} (0.060 nm) and the absorption peaks we can conclude that the Co atomically substitutes on Zn sites. This is also confirmed in many groups, which included a variety of methods and optical absorption [15,18,20–22].

The optical transmission spectrum can be used in the determination of the optical constants of the thin film deposited onto the transparent substrate. When the product of the refractive index and film thickness of the film have allowed the formation of interference fringes, classical methods such as the envelope method developed by Swanepoel [23] can be used. As well as the number of the interference fringes and depth of the fringes are crucial to perform this method. However, Pointwise Unconstrained Minimization Algorithm (PUMA) [24] and many other iterative methods [25] can be used when the interference fringes observed or not observed in the transmission spectrum. Considering the normal dispersion relation, the refractive index decreases with the increasing wavelength. This is not valid for the Co:ZnO thin films for the region where the loss of transmission due to Co^{2+} characteristic transitions which modulate the transmittance spectrum of our samples is observed. Therefore, we used PUMA technique for this limited region which starts from the inflexion wavelength to the wavelength corresponding first characteristic transition which is centered at 571 nm (2.18 eV). Inflexion wavelength is defined from second derivative of optical transmission curve [6,26]. There is an excellent agreement between the experimental spectra and theoretical spectra for all the samples and one of the experimental and computed optical transmission spectra for the Co:ZnO thin film are shown in Fig. 4. Calculated film thickness and refractive index for 532 nm are given in Table 2. The value of refractive index is passing through a maximum considering the Co concentration such as

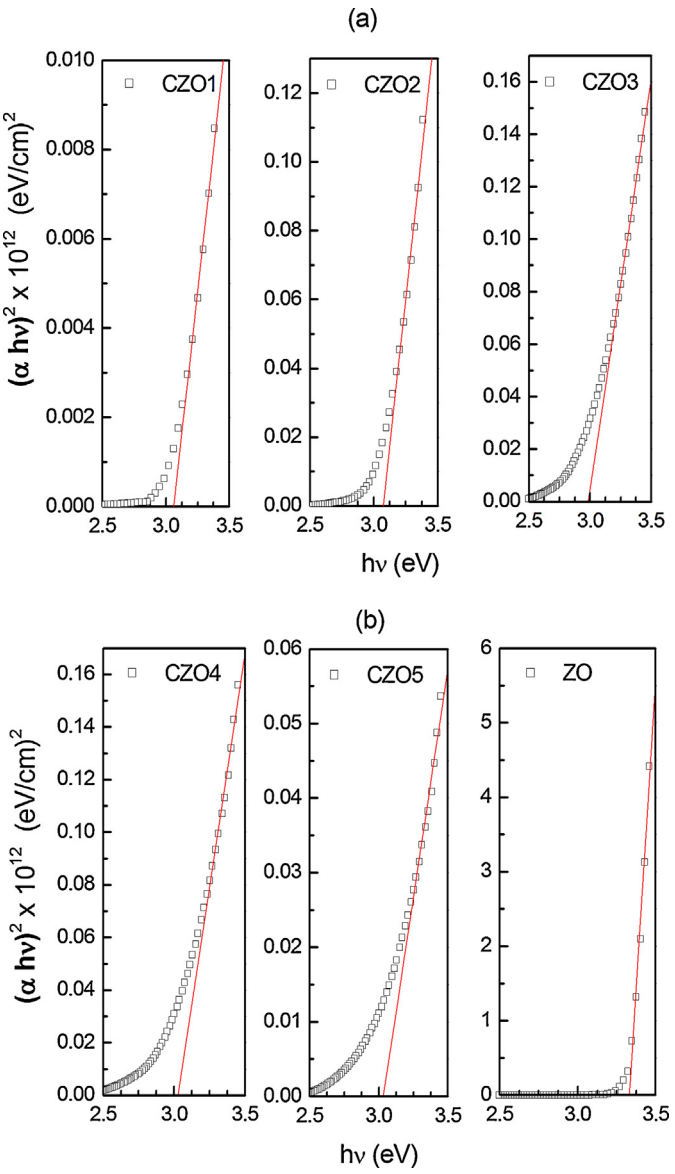

Fig. 5. Optical absorption spectra of the Co:ZnO and ZnO thin films as $(\alpha h\nu)^2 - h\nu$ behavior.

0.03 M. Then, the refractive index starts to decrease again. Having such a turning point is in agreement with the other observations such as XRD and PL measurements.

Not only the film thickness and refractive index but also optical absorption spectrum can be obtained from the optical transmission spectrum using suitable methods. Absorption edges for the semiconductors inform the threshold of charge transition between the highest filled band and the lowest empty band. The optical band gap of the films can be calculated using the following equation [27]:

$$\alpha h\nu = A(h\nu - E_g)^n \quad (1)$$

where A is the probability parameter for the transition, E_g is the band gap of the material, $h\nu$ is the incident photon energy, and n is the transition coefficient. The value of n is known:, 2 for the measurement of an indirect band gap and 1/2 for a direct band gap.

Fig. 5a–f shows the plot of $(\alpha h\nu)^2$ vs the photon energy $(h\nu)$ of the Co:ZnO thin films. The direct band gap of the films was determined by taking the intersection of the extrapolated lines from the linear vertical and horizontal regions near the band-edge of the $(\alpha h\nu)^2 = 0$ curve. As the Co concentration is increased in the ZnO

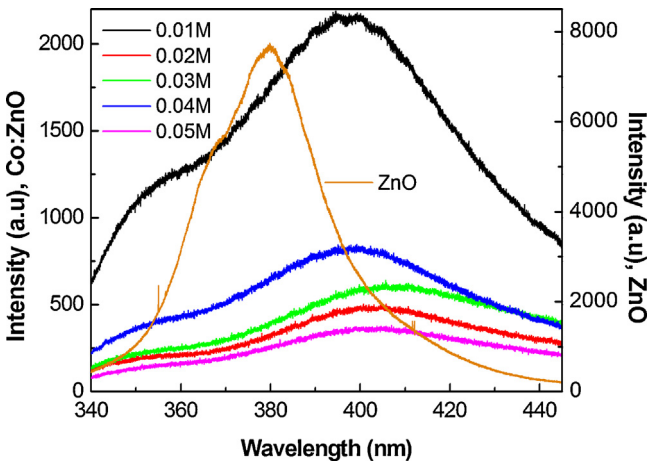

Fig. 6. PL spectra of Co:ZnO and ZnO thin films at room temperature.

Table 3
Photoluminescence (PL) analysis from Gaussian fitting process with two Gaussian peaks centered at λ_1 and λ_2 for samples, and computed optical band gap (E_g).

Molarity of Co (M)	λ_1 (nm)	λ_2 (nm)	E_g (eV)
0.00	379.65	–	3.26
0.01	390.95	407.41	3.17
0.02	397.64	415.20	3.12
0.03	401.87	417.93	3.09
0.04	389.01	406.93	3.18
0.05	396.18	412.80	3.13

structure, red shift is observed in the absorption edge due to the *sp-d* exchange interactions between the band electrons and the localized *d*-electrons of the Co^{2+} ions substituting Zn^{2+} ions. Calculated value of the optical band gap with increasing Co molarity from 0 to 0.05 M is given in Table 1.

Fig. 6 shows the PL spectra of as-grown samples. Photoluminescence spectra of the samples have been recorded at room temperature. The PL emission in the UV bands was observed. Band-edge transitions as well as direct-band transitions for ZnO at around 380 nm (3.26 eV) are observed. Gaussian fitting was performed on the PL spectra of the samples containing Co. Among the two peaks one is centered around 400 nm (λ_1) assigned to the band gap transition and the other peaks assigned to the near-band-edge (NBE) emission are centered at 407 nm, 415 nm, 418 nm, 407 nm and 413 nm for the samples CZ01, CZ02, CZ03, CZ04 and CZ05, respectively (Table 3). Band gap values are decreasing up to a threshold value of Co concentration. This behavior is also observed in the refractive index variation. In addition, the observed PL intensity began to decrease when the cobalt was introduced into the ZnO structure.

4. Conclusion

The structure and optical properties of Co doped ZnO films were studied with respect to cobalt concentration in the starting solution in which the cobalt acetate tetrahydrate was used as a Co source. Our studies show that Co doping affects ZnO lattice immediately. When the Co molarity is greater than the 0.03 M or Co concentration obtained from EDS analysis is about 12%, the ZnO (0 0 2) peak intensity decreases and CoO (2 0 0) peak intensity increases with increasing Co concentration. Co substitution in ZnO lattice has been proved by the optical transmittance measurement, whereas it is not clearly seen in the XRD diffractogram for the CZO1 and CZO2 sample. The optical transmittance decreases with increasing Co concentration. ZnO is white colored because it does not absorb any

visible light. When the Zn^{2+} ions are replaced with Co^{2+} ions in the ZnO lattice, the films absorb visible light, and the color of the films turn to deep green. The character of the band gap of the CZO films is direct type with cobalt doping. When the cobalt doping is increased, Tauc plots are becoming a more rounded in shape and the inflexion point moves to the longer wavelengths. The band gap obtained from Tauc's plot shifting toward to the longer wavelengths was verified with room temperature PL measurement. The band gap narrowing can be attributed that the conduction band and the valence band shifted downward and upward, respectively. We concluded that the red-shift is typically attributed to the *sp–d* exchange between the ZnO band electrons and localized *d*-electrons associated with the doped Co^{2+} cations.

Acknowledgement

This study was supported by The Scientific Research Unit of Mehmet Akif Ersoy University with project numbers 110-NAP-10, 0172-NAP-13, and 0173-NAP-13.

References

[1] M.G. Tsoutsouva, C.N. Panagopoulos, D. Papadimitriou, I. Fasaki, M. Kompitsas, ZnO thin films prepared by pulsed laser deposition, Mater Sci Eng B 176 (6) (2011) 480–483.
[2] S. Kumar, Y.J. Kim, B.H. Koo, H. Choi, C.G. Lee, Ferromagnetism in chemically-synthesized Co-doped ZnO, J. Korean Phys. Soc. 55 (3) (2009) 1060–1064.
[3] M. Harati, D. Love, W.M. Lau, Z. Ding, Preparation of crystalline zinc oxide films by one-step electrodeposition in Reline, Mater Lett 89 (2012) 339–342.
[4] S. Vempati, A. Shetty, P. Dawson, K.K. Nanda, S.B. Krupanidhi, Solution-based synthesis of cobalt-doped ZnO thin films, Thin Solid Films 524 (2012) 137–143.
[5] S. Karamat, R.S. Rawat, T.L. Tan, P. Lee, S.V. Springham, R. Anis-ur-Rehman, H.D. Chen, Sun, Exciting dilute magnetic semiconductor: copper-doped ZnO, J. Supercond. Nov. Magn. 26 (2013) 187–195.
[6] E. Gungor, T. Gungor, Effect of the substrate movement on the optical properties of ZnO thin films deposited by ultrasonic spray pyrolysis, Adv. Mater. Sci. Eng. (2012), article ID: 594971 (7 pages).
[7] M. Tay, Y. Wu, G.C. Han, T.C. Chong, Y.K. Zheng, et al., Ferromagnetism in inhomogeneous $Zn_{1-x}Co_xO$ thin films, J Appl Phys 100 (2006) 063910.
[8] T. Dietl, H. Ohno, F. Matsukura, J. Cibert, D. Ferrand, Zener model description of ferromagnetism in zinc-blende magnetic semiconductors, Science 287 (2000) 1019–1022.
[9] K. Sato, H. Katayama-Yoshida, Material design for transparent ferromagnets with ZnO-based magnetic semiconductors, Jpn. J. Appl. Phys. Pt. 2 (39) (2000) L555–L558.
[10] K. Sato, H. Katayama-Yoshida, Stabilization of ferromagnetic states by electron doping in Fe-, Co- or Ni-doped ZnO, Jpn. J. Appl. Phys. Pt. 2 (40) (2001) L334–L336.
[11] K.J. Kim, Y.R. Park, Spectroscopic ellipsometry study of optical transitions in $Zn_{1-x}Co_xO$ alloys, Appl Phys Lett 81 (2002) 1420.
[12] M. Bouloudenine, N. Viart, S. Colis, A. Dinia, Bulk $Zn_{1-x}Co_xO$ magnetic semiconductors prepared by hydrothermal technique, Chem Phys Lett 397 (2004) 73–76.
[13] S.V. Bhat, F.L. Deepak, Tuning the bandgap of ZnO by substitution with Mn^{2+}, Co^{2+} and Ni^{2+}, Solid State Commun 135 (2005) 345–347.
[14] X. Liu, E. Shi, Z. Chen, H. Zhang, L. Song, H. Wang, S. Yao, Structural, optical and magnetic properties of Co-doped ZnO films, J Cryst Growth 296 (2006) 135–140.
[15] M. Ivill, S.J. Pearton, S. Rawal, L. Leu, P. Sadik, R. Das, A.F. Hebard, M. Chisholm, J.D. Budai, D.P. Norton, Structure and magnetism of cobalt-doped ZnO thin films, New J. Phys. 10 (2008) 065002.
[16] H.-J. Lee, S.H. Choi, C.R. Cho, H.K. Kim, S.-Y. Jeong, The formation of precipitates in the ZnCoO system, Europhys Lett 72 (1) (2005) 76–82.
[17] M. Bouloudenine, N. Viart, S. Colis, J. Kortus, A. Dinia, Appl Phys Lett 87 (2005) 052501.
[18] C.B. Fitzgerald, M. Venkatesan, J.G. Lunney, L.S. Dorneles, J.M.D. Coey, Cobalt-doped ZnO at room temperature dilute magnetic semiconductor, Appl Surf Sci 247 (2005) 493–496.
[19] C. Rath, S. Singh, P. Mallick, D. Pandey, N.P. Lalla, N.C. Mishra, Effect of cobalt substitution on microstructure and magnetic properties in ZnO nanoparticles, Indian J. Phys. 83 (4) (2009) 415–421.
[20] A.C. Tuan, et al., A.C. Tuan, J.D. Bryan, A.B. Pakhomov, V. Shutthanandan, S. Thevuthasan, D.E. McCready, D. Gaspar, M.H. Engelhard, J.W. Rogers Jr., K. Krishnan, D.R. Gamelin, S.A. Chambers, Epitaxial growth and properties of cobalt-doped ZnO on alpha-Al_2O_3 single-crystal substrates, Phys Rev B 70 (2004) 054424.
[21] C. Song, F. Zeng, K.W. Geng, X.B. Wang, Y.X. Shen, F. Pan, The magnetic properties of Co-doped ZnO diluted magnetic insulator films prepared by direct current reactive magnetron co-sputtering, J Magn Magn Mater 309 (2007) 25–30.
[22] K. Samanta, P. Bhattacharya, R.S. Katiyar, Optical properties of $Zn_{1-x}Co_xO$ thin films grown on Al_2O_3 (0 0 0 1) substrates, Appl Phys Lett 87 (2005) 101903.
[23] R. Swanepoel, Determination of the thickness and optical constants of amorphous silicon, J. Phys. E.: Sci. Instrum. 16 (1983) 1214–1222.
[24] E.G. Birgin, I. Chambouleyron, J.M. Martinez, Estimation of optical constants of thin films using unconstrained optimization, J. Comput. Phys. 151 (1999) 862–888.
[25] T. Güngör, B. Saka, Calculation of the optical constants of a thin layer upon a transparent substrate from the reflection spectrum using a genetic algorithm, Thin Solid Films 467 (2004) 319–325.
[26] R. Dolbec, M.A. El Khakani, A.M. Serventi, M.T. Rudeau, R.G. Saint-Jacques, Microstructure and physical properties of nanostructured tin oxide thin films grown by means of pulsed laser deposition, Thin Solid Films 419 (2002) 230–236.
[27] J. Tauc, R. Grigorovici, A. Vancu, Optical properties and electronic structure of amorphous germanium, Phys. Stat. Solidi 15 (1966) 627.